A Numerical/Experimental Study of Nitinol Actuator Springs

Ferdinando Auricchio
DICAr, Università di Pavia, Pavia, Italy - auricchio@unipv.it

Giulia Scalet
DICAM, Università di Bologna, Bologna, Italy - giulia.scalet2@unibo.it

Marco Urbano
SAES Getters S.p.A, Lainate, Milano, Italy - marco_urbano@saes-group.com

Abstract

The present study deals with the numerical modeling, simulation and experimental analysis of shape memory alloy (SMA) helicoidal springs. An experimental campaign is conducted on both SMA straight wires and helicoidal springs that experienced the same annealing process. Then, we use such experimental results to investigate three phenomenological constitutive models able to represent SMA macroscopic behavior. In particular, after the identification of all the material parameters from experimental results on SMA wires, we inspect the thermo-mechanical behavior of SMA helicoidal springs by comparing numerical predictions to experimental data. Finally, we discuss models capabilities and some aspects characterizing SMA material behavior.

Keywords

shape memory alloys, helicoidal springs, numerical modeling, experimental tests

1 Introduction

Shape memory alloys (SMAs), belonging to the class of smart materials, are exploited in a variety of interesting applications. Solid phase transformations, induced either by stress or temperature, are behind the remarkable functional properties of SMAs, promoting the concept of innovative smart actuators. SMA helicoidal springs are devices that combine an actuator, a sensor (typically a temperature sensor), and a displacement amplifier. A single component is indeed a system able to accomplish complex functions, as reacting to a temperature variation with an actuation. Despite the apparent simplicity, the behavior of SMA helicoidal springs is rather complex due to SMA thermo-mechanical properties. Consequently, the development process of such devices is a difficult task and their design may possibly take advantage of numerical simulations.

The literature presents numerous efforts for the modeling, design, simulation and control of SMA actuator systems [1, 2]. Among them, some works present different spring modeling approaches and calibration techniques to model the thermo-mechanical behavior of SMA helicoidal springs [3-9]. For instance, the paper by Attanasi et al. [9] investigates SMA spring superelastic mechanical behavior in tension and compression through some experimental and numerical analyses. Springs are modeled using two-node simple beam elements and material properties are computed through a trial and error fitting process on several experimental data related to a spring specimen. The paper by Dumont and Kühl [3] proposes a finite element (FE) model of the Euler-Bernoulli beam and a material parameters identification on experimental data related to SMA wires. Aguiar et al. [5] assume a 1D constitutive model to describe SMA thermo-mechanical shear behavior and a classical approach for linear-elastic springs. Toi et al. [6] extend Brinson's 1D constitutive modeling to consider the asymmetric tensile and compressive behavior as well as the torsional behavior of superelastic, large deformation analysis of SMA springs. The authors formulate the FE method using linear Timoshenko beam elements. The work by Saleeb et al. [8] focuses on the characterization of the cyclic behavior of 55NiTi using a new modeling framework and its 3D FE implementation applied to springs. Model calibration is based on a single thermal-cycling test at constant load on a SMA wire.

However, computational methods have not yet been well established for the analysis of SMA springs [10, 11], particularly, in relation to the aim of finding an accurate FE modelization of spring devices, an appropriate SMA constitutive model as well as a simple calibration technique.

Motivated by these considerations, the present paper focuses on the investigation of SMA helicoidal spring actuator behavior, by combining the results of an experimental campaign conducted in Saes Getters with a thorough understanding of SMA experimental behavior and the selection of appropriate constitutive models.

More specifically, the purpose of the present work is to investigate reliable and exhaustive SMA 3D constitutive models which could be used by engineers needing to perform accurate simulations for the design and study of the response of SMA structures or components, in particular of SMA helicoidal springs. To reach this goal, the considered models have to be interfaced with commercial analysis programs; accordingly, good models should also be robust and flexible, possibly including both superelasticity and shape-memory effect, without increasing modeling complexity. Also, the problem of the physical interpretation of the model parameters is an important issue, as a clear and effective parameter identification procedure is the key for the employment of a constitutive model by engineers in real-life simulations.

Among the several models available in the recent literature, the present work focuses on three different SMA macroscopic constitutive models; in particular, on **(i)** the model by Souza et al. [12] and then investigated by

Auricchio and Petrini [13]; **(ii)** the model by Auricchio et al. [14, 15]; and **(iii)** the model by Auricchio and Bonetti [16] and then investigated by Auricchio et al. [17].

The investigation of the three models is based on a comparison between numerical predictions and experimental data. Such data are obtained by an experimental campaign conducted in Saes Getters on both SMA straight wires and helicoidal springs that experienced the same annealing process and presenting different geometries. The conducted tests consist of two experimental temperature loops at different constant tensile loads, carried out on wires and springs. Accordingly, the main goal of the present work is to calibrate constitutive model parameters on some experimental results related to SMA wires and then to test the resulting models with experimental data on helicoidal springs. The comparison between numerical predictions and experimental results allows to make considerations on the models reliability and design aspects as well as to discuss some features of SMA material behavior, highlighted by the experimental campaign.

In the following, we briefly show and comment basic model properties. Then, we describe the calibration process of constitutive model parameters and we compare numerical predictions to experimental data on helicoidal springs. Finally, we conclude by discussing and commenting the obtained results.

2 Model properties review

This Section briefly reviews the principal features and differences between the 3D phenomenological constitutive models investigated in the present study, e.g., the Souza-Auricchio [12, 13], modified Souza-Auricchio [14, 15], and Auricchio-Bonetti [16, 17] models. For a more detailed presentation, the reader is referred to the works [12-17].

The first investigated model has been originally presented by Souza et al. [12] and then investigated by Auricchio and Petrini [13]. Therefore, in the following we refer to this model as the *Souza-Auricchio model*.

The model has been recognized as very effective in capturing main SMA macroscopic features, especially in consideration of the limited number of involved parameters. This model is in fact able to describe both superelasticity and shape-memory effect by assuming the transformation strain, associated to transformations between austenite and single-variant martensite, as tensorial internal variable. The model has been treated numerically by Auricchio and Petrini [13]. The solution algorithm is simple and robust as it is based on a plasticity-like return map procedure and makes the model suitable for implementation within FE codes, allowing the simulation of complex SMA devices.

The Souza-Auricchio model [12, 13] presents, however, some limitations, e.g., in properly capture low stress phase transformations, as often required by industrial applications [14]. The model can be extended as done by Auricchio

et al. [14, 15], through the introduction of a linear dependence of the elastic radius on temperature to improve model capability to catch the transition phase for low stress phase transformations. Therefore, in the following we refer to this model as the *modified Souza-Auricchio model*. The same numerical treatment of the Souza-Auricchio model has been adopted for the modified Souza-Auricchio model [14, 15].

Further improvements can be obtained by extending the model as theoretically done by Auricchio and Bonetti [16] and then generalized by Auricchio et al. [17], i.e., including effects such as martensite reorientation, different kinetics between forward/reverse phase transformations, smooth thermo-mechanical response, low-stress phase transformations as well as transformation-dependent elastic properties. In particular, the theoretical framework allows for a completely independent description of the different phase transformations, leading to a very flexible frame in terms of model features. Therefore, in the following we refer to this model as the *Auricchio-Bonetti model*.

The model introduces scalar and tensorial internal variables. In particular, volume proportions of different configurations of crystal lattice (i.e., austenite, single- and multiple-variant martensites) are used as scalar internal variables and the direction of single-variant martensite as tensorial internal variable. The algorithmic treatment of model equations, presented by Auricchio et al. [17], consists in replacing the Kuhn-Tucker conditions by the equivalent Fischer-Burmeister complementarity function. The application of the Fischer-Burmeister function makes possible to omit an active set search, a fundamental advantage when dealing with many coupled evolution equations.

3 Experimental campaign

This Section presents the experimental campaign conducted in SAES Getters.

Experiments consisted in thermal cycling at constant tensile load and were performed on the following samples:

- 1.5 mm diameter straight annealed wires;
- 1.0 mm diameter straight annealed wires;
- helicoidal springs manufactured by shape setting of either 1.5 mm and 1.0 mm diameter cold drawn wires.

All samples material nominal composition was Ti-49Ni at%.

The geometrical parameters of the two spring configurations are reported in Tables 1 and 2.

Table 1. Geometrical parameters of the first helicoidal spring actuator (Actuator 1).

Wire diameter	1.5 mm
External coil diameter	13.3 mm
Pitch	6.4 mm
Free coils	3.5

Initial length	24.59 mm

Table 2. Geometrical parameters of the second helicoidal spring actuator (Actuator 2).

Wire diameter	1.0 mm
External coil diameter	7.5 mm
Pitch	3.0 mm
Free coils	6
Initial length	18.0 mm

The shape setting processes of both spring versions were conducted with identical process parameters.

Wires heat treatment were performed so that the wire experienced the same temperature time evolution of the corresponding spring.

All thermal cycling tests were carried out on a self-constructed measuring system, already described in [19]. The system was recently provided with a thermostatic chamber featuring a temperature range from less than -100°C to more than 350°C. The chamber is made of an inner brass chamber. Inside its walls holes for Nitrogen flow and resistive heaters are drilled. The brass chamber is contained is a two layers thermal insulation case, the inner layer having high temperature stability, the outer layer good structural capability. Temperature inside the thermostatic chamber is monitored by means of three thermocouples, one of which, placed more or less in the center of the free volume and very close to the sample, is utilized for feedback control. A fan inside the chamber contributes to homogenize the temperature profile.

Temperature and displacement were registered during the tests. The displacement was measured by means of the encoder of the linear motor exerting the load, properly corrected to compensate for thermal dilatation and elastic elongation of the loading chain.

Thermal cycling was run on each SMA sample, either wire or spring, with increasing load. Two thermal cycles, starting from the high temperature, were performed for each load. Figure 1 shows the springs before and after testing and Table 3 summarizes all the performed tests.

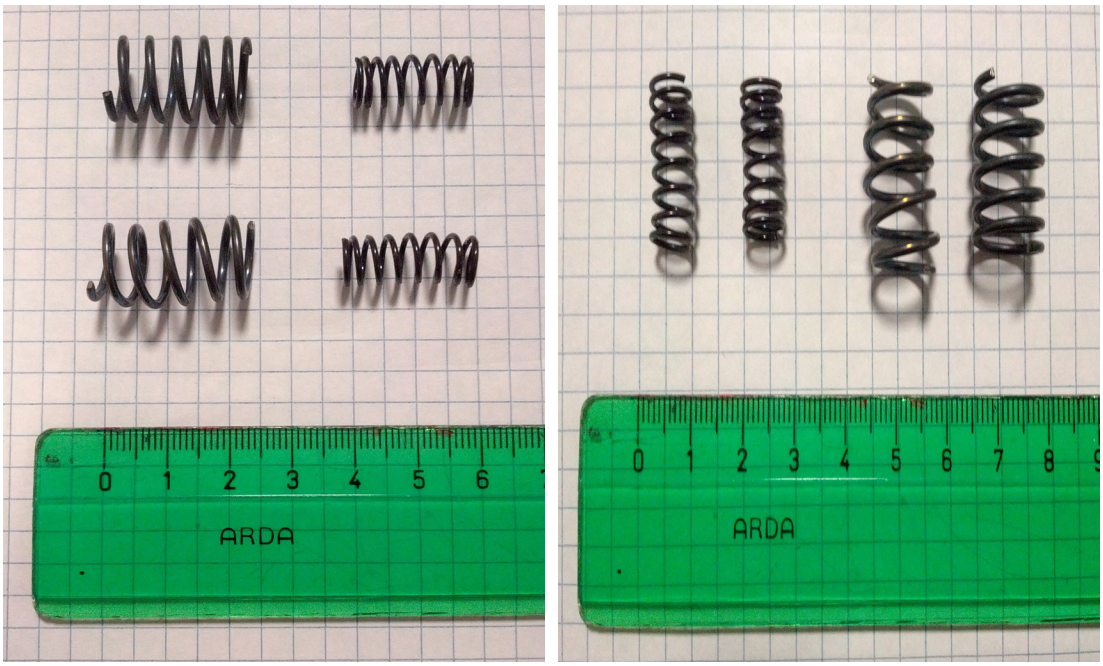

Figure 1. Springs before and after testing.

Table 3. Summary of the performed tests in SAES Getters.

Component	Loads	Thermal Cycles for each load
1.0 mm diameter wire	15 MPa, 30 MPa, 50 MPa, 100 MPa, 200 MPa	2
1.5 mm diameter wire	55 MPa, 100 MPa, 144 MPa	2
Spring 1	3 N, 5 N, 8 N	2
Spring 2	1 N, 2 N, 5 N, 7 N	2

4 Parameter identification procedure

This Section is dedicated to the calibration of the investigated models. Ideally, the calibration procedure of a comprehensive material model with an extensive amount of experimental data on SMA springs should be automated using sophisticated optimization techniques. In the present work, however, the identification of all the material parameters is based on two experimental thermal-cycling tests at constant load conducted on a SMA wire. We consider these kind of experimental results, instead of classical stress-strain curves, because the strain-temperature response is very significant for SMA producers, being one of the most important characteristic of SMA for actuators.

In particular, the calibration technique is achieved through a comparison between the two experimental curves in a 1D setting, as already done for the Souza-Auricchio model by Auricchio et al. [14]. Consequently, we easily calibrate the following parameters of the Souza-Auricchio model: **(i)** the elastic properties (E and ν), **(ii)** the

maximum amount for single-variant martensite (e_L), and **(iii)** four additional parameters (R, h, b, and T_0) characteristic of martensitic transformations. **We remark that, since the performed tests are under tensile load, we take a typical approximate value of the Poisson's ratio from literature [20].**

Then, we adopt the same values for the parameters of the modified Souza-Auricchio model, except for the radius, R_1, assumed equal to R, and for the radius, R_0, calibrated to catch material behavior for low stress conditions. Finally, we adopt the same elastic properties (E and n) and the same maximum amount for single-variant martensite (e_L) for the Auricchio-Bonetti model and we calibrate the remaining parameters (i.e., Y^{in}, Ds^{ASM}, R^M, R^S_f , R^S_r, h^S_f, h^S_r, and T_0), through a comparison between the two experimental curves in a 1D setting as described by Auricchio et al. [17].

We remark that the above calibration process is based on the results of tensile tests under the hypothesis of isotropic material response and tension-compression symmetry, since we are interested in catching the global material behavior. Thus, we do not capture important features for drawn NiTi wires as the effects of tension-compression asymmetry and of material texture which may strongly influence the yield transformation surfaces and the transformation strains. In such a case, a multiaxial characterization of NiTi wires would be appropriate, although difficult.

For the identification procedure, we use the 100 and 144 MPa curves related to the 1.5 mm wire. Table 4 lists the values of the parameters adopted in all the numerical simulations (already reported to a 3D setting) and Figures 2(a)-(c) present the 1D phase diagrams for the three models in terms of stress, s, and temperature, T.

Table 4. Calibrated material parameters for the three models.

Souza-Auricchio model	Mod. Souza-Auricchio model	Auricchio-Bonetti model
E = 45000 MPa n = 0.3 e_L = 0.049 T_0 = 343 K R = 110 MPa h = 1000 MPa b = 4.49 MPa/K	E = 45000 MPa n = 0.3 e_L = 0.049 T_0 = 343 K R_1 = 110 MPa R_0 = 10 MPa h = 1000 MPa b = 4.49 MPa/K	E = 45000 MPa n = 0.3 e_L = 0.049 T_0 = 325 K R^M = 1 MPa R^S_f = 2.4 MPa R^S_r = 8 MPa h^S_f = 1.3 MPa h^S_r = 2.0 MPa Y^{in} = 0.25 MPa Ds^{ASM} = 0.2 MPa/K

As it can be observed from Figures 2(a) and 2(b), the Souza-Auricchio and the modified Souza-Auricchio models consider the coexistence of only two phases, i.e., austenite and single-variant martensite, and differ from each other for material behavior at low temperatures, i.e., at $T < T_0$, where T_0 is assumed equal to 70 °C. In particular, the modified Souza-Auricchio model considers a lower value of the elastic radius than the Souza-Auricchio model, i.e., $R_0 = 10$ MPa, which allows to take into account temperature transformations at low levels of stress. The Auricchio-Bonetti model considers also the presence of multi-variant martensite, consequently taking into account thermal-induced transformations at zero stress (indicated by vertical red dot lines in Figure 2(c)).

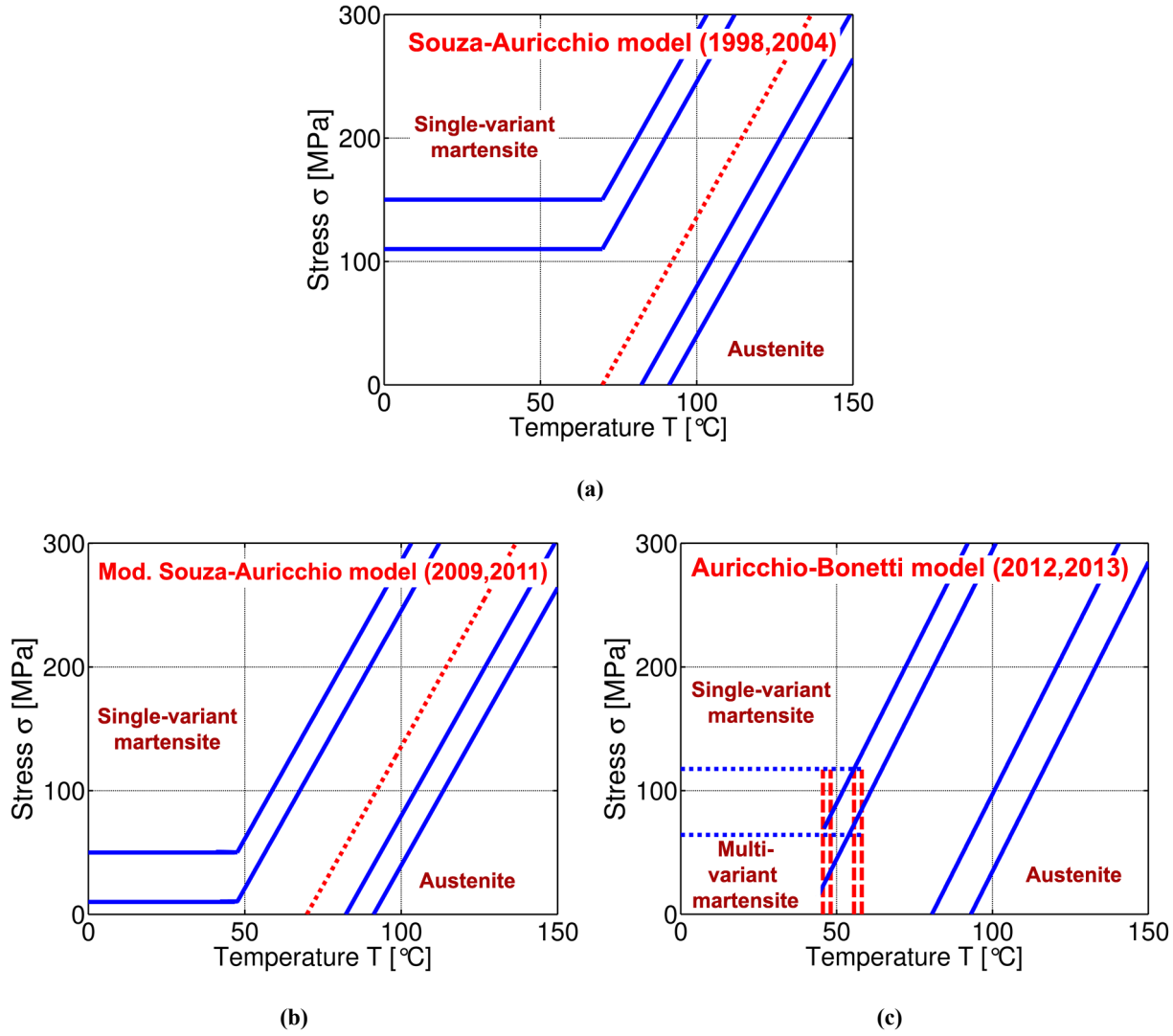

Figure 2. 1D phase diagrams generated by (a) the Souza-Auricchio model; (b) the modified Souza-Auricchio model and (c) the Auricchio-Bonetti model, in terms of stress, s, and temperature, T.

With the calibrated parameters of Table 4, we produce the numerical curves for the 100 and 144 MPa cases, to compare with the experimental curves from which the parameters have been identified. Such numerical curves have been obtained in two Mathematica FE packages, AceGen and AceFEM [18], by simulating the experimental thermal-cycling tests at constant load as uniaxial tension tests with load control and prescribed homogeneous varying temperature field.

Figure 3 reports the comparison between the experimental and the calibrated curves in terms of strain, e, and temperature, T, for the two levels of load. In this and in the following figures, we refer to the Souza-Auricchio model as **SA**, to the modified Souza-Auricchio model as **mod. SA**, and to the Auricchio-Bonetti model as **AB**.

In particular, Figure 3 shows the inability of the Souza-Auricchio model to catch SMA behavior for work conditions where the material is considered as linear elastic and where the model is particularly sensitive to its numerical implementation. Given the assessed material coefficient set, such a work condition includes stress values approximately lower than 150 MPa at $T < T_0$, as it can be observed in Figure 2(a). The applied experimental loads belong exactly to such a stress range, causing the inefficiency of the Souza-Auricchio model. Contrarily, the modified Souza-Auricchio and Auricchio-Bonetti models demonstrate their efficiency in capturing real material response.

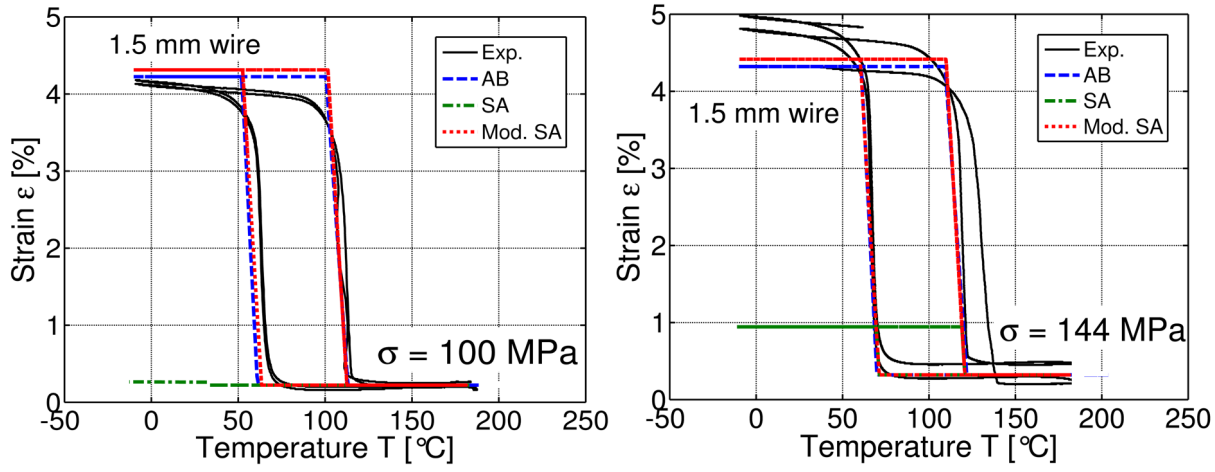

Figure 3. Parameters identification on thermal-cycling tests on 1.5 mm SMA wires.

Deformation, e, vs. temperature, T, curves at constant tensile loads of 100 and 144 MPa.

5 Comparison with experimental data on SMA helicoidal springs

This Section presents the comparison between experimental data and numerical predictions on SMA helicoidal springs presenting different geometries. Experimental tests have been carried out in SAES Getters, as described in

Section 3. Numerical results are obtained by conducting 3D FE analyses of SMA helicoidal springs subjected to temperature cycling at constant load with the material parameters presented in Table 4. We remark that the aim of the present work is to show as the three models catch SMA experimental behavior with a simple calibration process. Consequently, all the studied experimental data-sets are simulated with a unique choice of material parameters, obtained with the calibration procedure described in Section 4. The material parameters calibrated on 1.5 mm wires are so employed in the analysis of 1.0 mm wires.

In the following, we present the results of FE analyses on 1.5 and 1.0 mm wire springs and, then, we report some considerations about model results and SMA experimental behavior.

5.1 Results for 1.5 mm wires and 1.5 mm wire springs

First, we present thermal-cycling tests at constant load on a 1.5 mm wire, simulated as uniaxial tension tests with load control and prescribed homogeneous varying temperature field. Figure 4 reports the comparison between experimental and numerical curves in terms of deformation, e, and temperature, T, for a tensile load of 55 MPa.

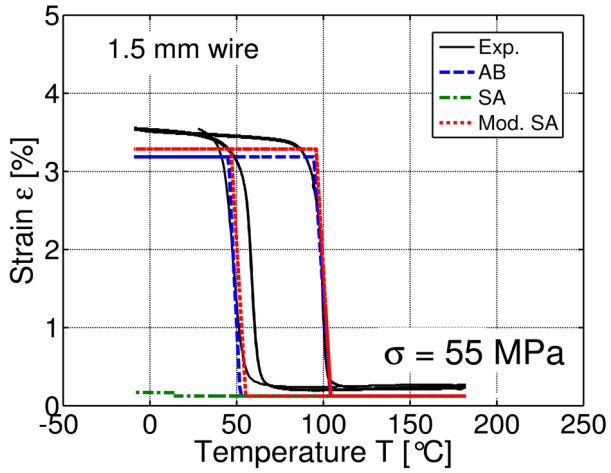

Figure 4. Thermal-cycling test on 1.5 mm SMA wire.

Deformation, e, vs. temperature, T, curves at constant tensile load of 55 MPa.

Then, we consider the FE analysis of a SMA helicoidal spring actuator (Spring 1 of Table 3). The adopted mesh consists of 6912 8-node brick elements and 7497 nodes (see Figure 5).

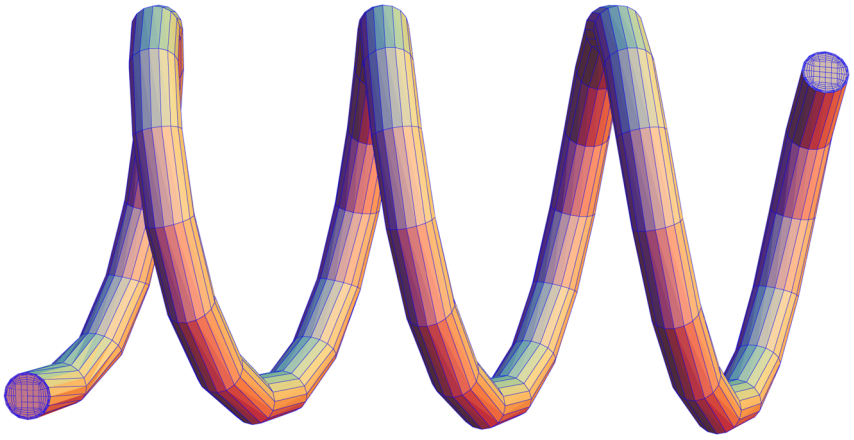

Figure 5. Adopted mesh for Spring 1 of Table 3.

We consider the spring fixed at the top end, initially loaded by an axial force at the bottom end and then, keeping constant the load, subjected to temperature cycle. We apply three forces of 3, 5 and 8 N. We remark that all the nodes on the bottom section are constrained against the two translations in the directions orthogonal to the axial one (thus ensuring that the bottom section is restrained against twist rotation). Moreover, we observe that the magnitudes of the three forces produce average values of approximately 33, 55, and 88 MPa for the distribution of effective stresses ($\sqrt{3}/2\mathbf{s}:\mathbf{s}$, where $\mathbf{s}$ is the stress deviator tensor) in SMA coils. This provides a comparable stress level to that utilized in the experiments used for characterization and calibration described in Section 4.

Figure 6 shows the spring relative elongation, $(L - L_0) / L_0$, versus temperature, T, diagrams, where L_0 is the initial length of the spring.

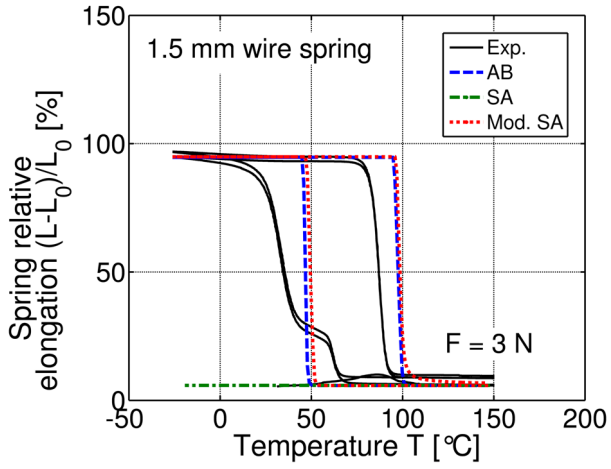

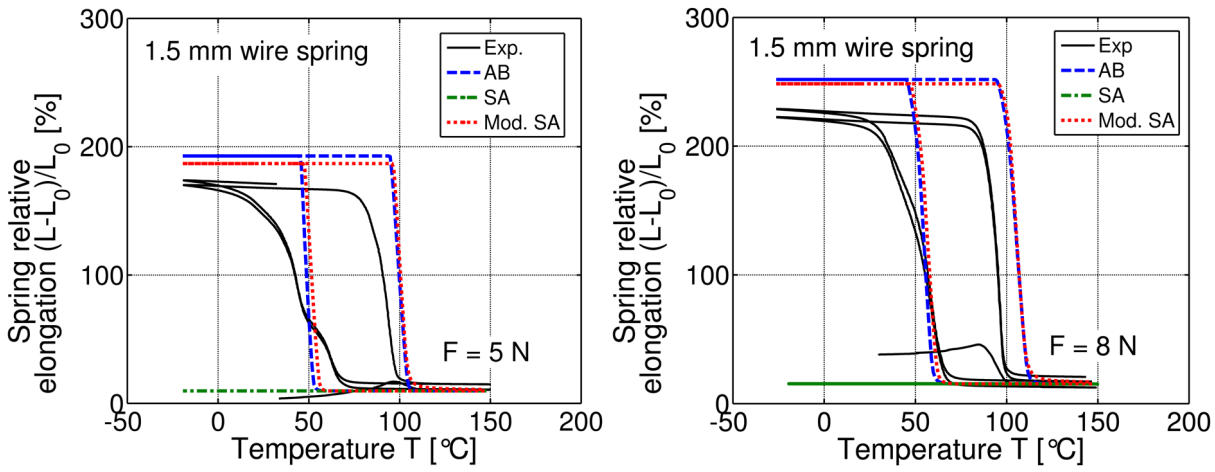

Figure 6. Thermal-cycling tests on 1.5 mm wire springs.

Spring relative elongation, (L - L_0) / L_0, vs. temperature, T, curves at constant loads of 3, 5 and 8 N.

5.2 Results for 1.0 mm wires and 1.0 mm wire springs

First, we present thermal-cycling tests at constant load on a 1.0 mm wire. We consider simulations of thermal-cycling tests at constant loads of 15, 30, 50, 100, and 200 MPa. Figure 7 reports e-T diagrams for the five levels of loads.

Then, we consider the FE analysis of a SMA helicoidal spring actuator (Spring 2 of Table 3). The adopted mesh consists of 14976 8-node brick elements and 16511 nodes (see Figure 8). In this case, we consider four force values of 1, 2, 5, and 7 N, whose magnitudes produce average values of approximately 23, 46, 115, and 161 MPa for the distribution of effective stresses in SMA coils. Figure 9 shows spring relative elongation, (L - L_0) / L_0, versus temperature, T, diagrams.

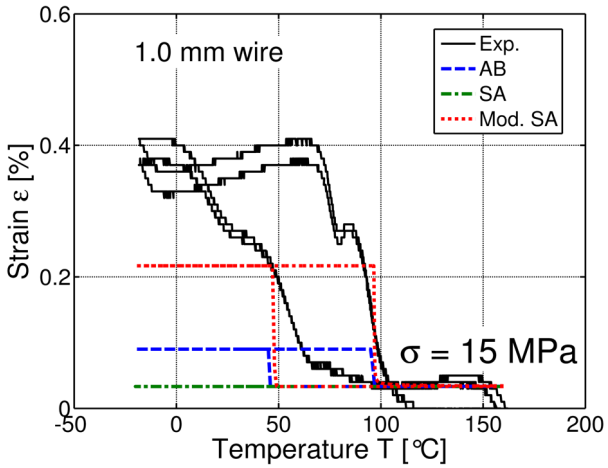

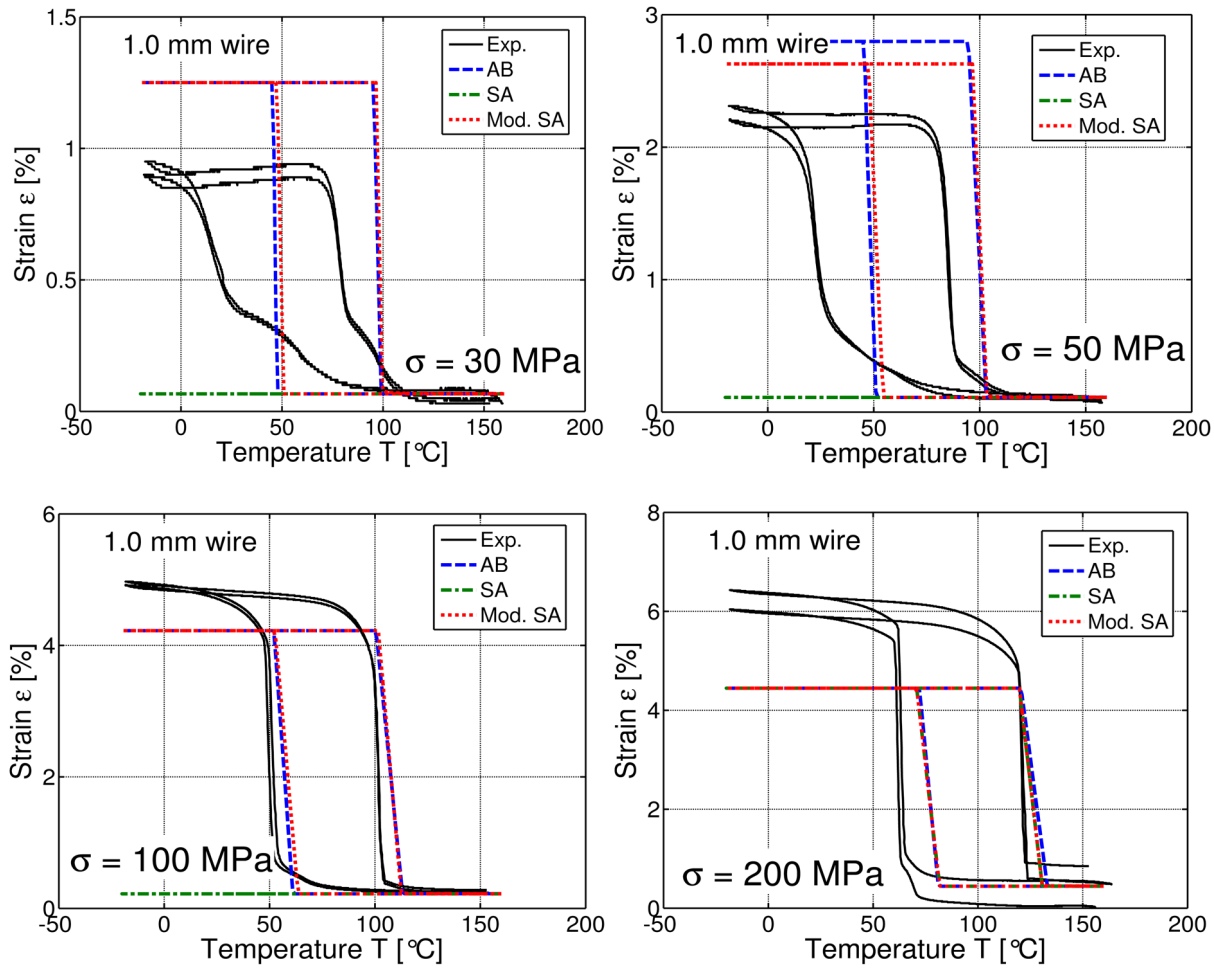

Figure 7. Thermal-cycling tests on 1.0 mm SMA wires.

Deformation, e, vs. temperature, T, curves at constant tensile loads of 15, 30, 50, 100, and 200 MPa.

5.3 Considerations

Numerical simulations show that the results of both the Auricchio-Bonetti and modified Souza-Auricchio models are almost the same and in close agreement with experimental data, revealing that the considered models capture the general thermo-mechanical behavior of SMA springs, notwithstanding the simple calibration process.

Starting from Figures 3, 4 and 6, referring to 1.5 mm wires and 1.5 mm wire springs, both the models catch successfully the experimental curves.

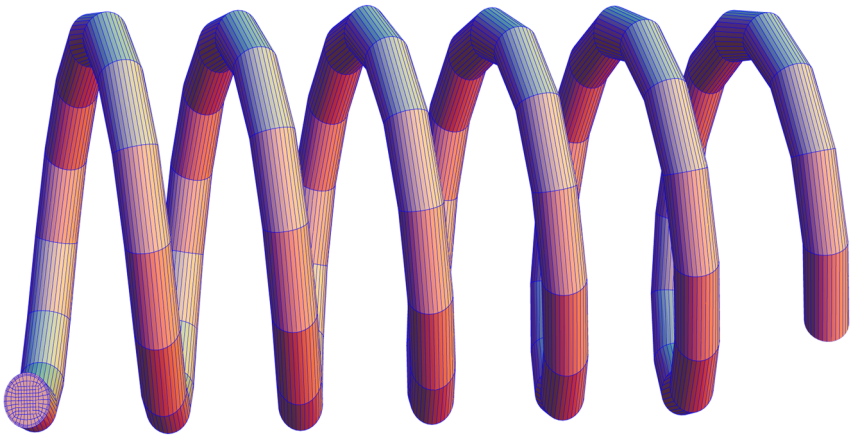

Figure 8. Adopted mesh for Spring 2 of Table 3.

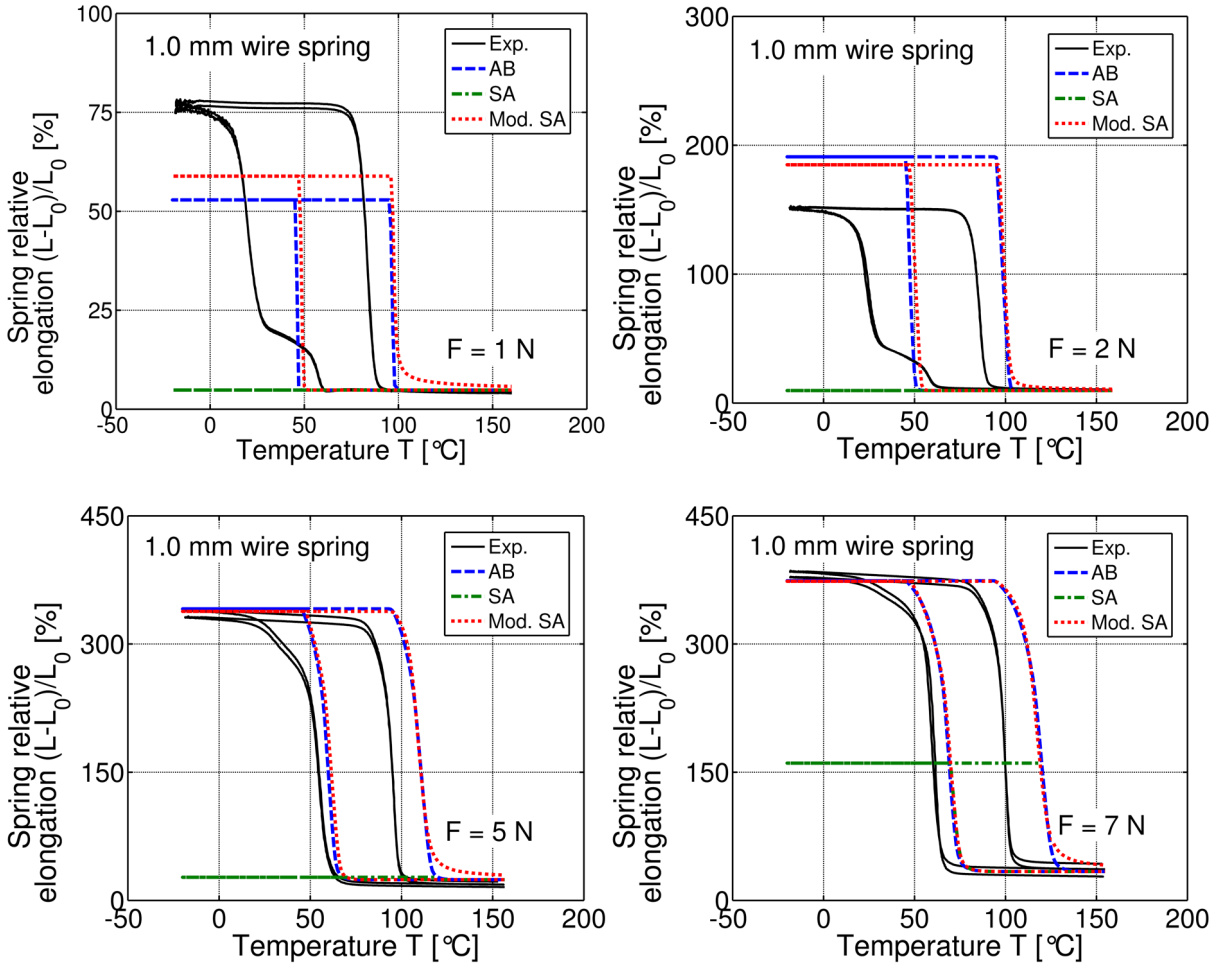

Figure 9. Thermal-cycling tests on 1.0 mm wire springs.

Spring relative elongation, (L - L_0) / L_0, vs. temperature, T, curves at constant loads of 1, 2, 5 and 7 N.

The effect of the variation of spring geometrical properties (e.g., diameter, number of coils, etc.) is then investigated by focusing on 1.0 mm wires and 1.0 mm wire springs. Numerical predictions related to 1.0 mm wires do not present satisfactory results, as shown in Figure 7. Experimental curves reveal, in fact, a significative influence of the variation of the diameter on SMA wire behavior, which is not taken into account by the uniaxial FE simulations. This can be observed by comparing, for instance, the experimental curves related to the applied load of 100 MPa for both the 1.5 mm and 1.0 mm wires (see Figures 3 and 7, respectively). Numerical curves are almost matching, while experimental ones differ for the values of the stroke and of the transformation temperatures.

Despite the poor matching for 1.0 mm wires, the results related to 1.0 mm wire springs are satisfactory in terms of the hysteresis loops, as reported in Figure 9, especially for the loads of 5 and 7 N, both generating high values of the effective stress. In fact, the two models do not match exactly the transformation temperatures. This issue could be related to the fact that material parameters have been calibrated on 1.5 mm wires and, in fact, experimental curves related to 1.5 mm wire springs are well described (see Figure 6).

Compared to the modified Souza-Auricchio model, the Auricchio-Bonetti model presents a more flexible approach, but also an increasing modeling complexity and a high number of material parameters. Moreover, the modified Souza-Auricchio model solves, with a low number of material parameters, the problem highlighted for the Souza-Auricchio model whose behavior depends on the numerical implementation.

As anticipated in Section 4, the Souza-Auricchio model does not catch successfully the experimental curves. This issue is related to the low values of the applied loads in experimental tests. In fact, starting from Figures 3, 4 and 6, referring to 1.5 mm wires and 1.5 mm wire springs, we observe the inability of the Souza-Auricchio model to catch SMA behavior for low work conditions. The results of the Souza-Auricchio model for 1.0 mm wires and 1.0 mm wire springs are not satisfactory too, as reported in Figures 7 and 9. In Figure 7, in fact, we observe that the only caught curve is that related to an applied load of 200 MPa. In Figure 9, the Souza-Auricchio model does not match the curve related to the load of 7 N, generating an approximate effective high stress of 161 MPa. This issue could be related to the numerical sensitiveness of the algorithm in the range of stresses lower or around 150 MPa and, in fact, the Souza-Auricchio model shows a starting transformation producing an uncompleted hysteresis loop.

Moreover, experimental curves highlight some characteristic features of SMA real behavior. As it can be observed in Figures 6, 7 and 9, the 1.5 mm wire springs, 1.0 mm wires and 1.0 mm wire springs reveal a double transformation transition due to the presence of the R-phase, particularly evident for low levels of stress. In Figure 7, related to 1.0 mm wires, such a transition takes place in the range of temperatures between 40 and 60 °C. Contrarily,

the 1.5 mm wires do not show any effect due to the R-phase, since their characterization involves high values of the load. Additionally, all the figures show irreversible strains.

6 Conclusions

This work has presented the numerical investigation of SMA actuator springs through the FE implementation of three macroscopic constitutive models. Comparison with experimental results has shown the inability of Souza-Auricchio model to catch SMA behavior for low levels of stress. Moreover, experimental curves have revealed the presence of some aspects characterizing SMA material behavior, as R-phase, plasticity, as well as training effects. Such effects are not accounted by the models. Despite this, the modified Souza-Auricchio and Auricchio-Bonetti models have revealed good predictions of global SMA behavior, by allowing to take advantage of these preliminary results for future design purposes. We remark, however, that the calibration process, adopted in the present work, requires the availability of experimental data on SMA wires for the identification of model parameters to be then used for spring simulations. **Thus, in order to make the calibration as easy as possible and to avoid a calibration process for each type of available wire, we have calibrated model parameters only on 1.5 mm wires.** Moreover, the calibration on data related to wires with specific geometries and material treatments are not well representative of all SMA wire springs. Despite this, the calibration is very simple compared to more sophisticated optimization techniques requiring large amount of experimental data and calculation time.

The present work will be used as a starting point for an ongoing detailed investigation about the calibration technique, the study of the effect of the variation of geometry properties and material treatment as well as of the application of compression loads.

7 Acknowledgements

The authors are grateful to Luca Fumagalli and coworkers for samples preparation, and to Alberto Coda and Andrea Cadelli for the experimental characterization.

References

[1] E.A. Khidir, N.A. Mohamed, M.J.M. Nor, M.M. Mustafa. A new method for actuating parallel manipulators. *Sensors Actuators A*, 2008, 147, 593-599.

[2] V. Bundhoo, E. Haslam, B. Birch, E.J. Park. A shape memory alloy-based tendon-driven actuation system for biomimetic artificial fingers, part I: design and evaluation. *Robotica*, 2009, 27, 131-146.

[3] G. Dumont, C. Kühl. Finite element simulation for design optimization of shape memory alloy spring actuators. *Eng. Comput.*, 2005, 22, 835-848.
[4] R.A.A. de Aguiar, W. de Castro Leo Neto, M. Savi, P. Calas Lopes Pacheco. Shape memory alloy helical springs performance: Modeling and experimental analysis. *Mater. Sci. Forum*, 2013, 758, 147-156.
[5] R.A.A. de Aguiar, M. Savi, P.M.C.L. Pacheco. Experimental and numerical investigations of shape memory alloy helical springs. *Smart Mater. Struct.*, 2010, 19, 1-9.
[6] Y. Toi, J.B. Lee, M. Taya. Finite element analysis of superelastic, large deformation behavior of shape memory alloy helical springs. *Comput. Struct.*, 2004, 82, 1685-1693.
[7] M.A. Savi, A.M.B. Braga. Chaotic vibrations of an oscillator with shape memory. *J. Braz. Soc. Mech. Sci. Eng.*, 1993, 15, 1-20.
[8] A. Saleeb, B. Dhakal, M. Hosseini, S. Padula II. Large scale simulation of NiTi helical spring actuators under repeated thermomechanical cycles. *Smart Mater. Struct.*, 2013, 22, 1-20.
[9] G. Attanasi, F. Auricchio, M. Urbano. Theoretical and Experimental Investigation on SMA Superelastic Springs. *J. Mater. Eng. Perform.*, 2011, 20 (4-5), 706-711.
[10] Y. Toi, J.B. Lee, M. Taya. Finite element analysis of superelastic behavior of shape memory alloy devices (part 1: small deformation analysis of tensile and bending behaviors). *Trans. Jpn Soc. Mech. Eng. A*, 2002, 68(676), 1688-1694, in Japanese.
[11] Y. Toi, J.B. Lee, M. Taya. Finite element analysis of superelastic behavior of shape memory alloy devices (part 2: finite deformation analysis of beams and helical springs). *Trans. Jpn Soc. Mech. Eng. A*, 2002, 68(676), 1695-1701, in Japanese.
[12] A.C. Souza, E.N. Mamiya, N. Zouain. Three-dimensional model for solids undergoing stress-induced phase transformations. *Eur. J. Mech. A-Solids*, 1998, 17, 789-806.
[13] F. Auricchio, L. Petrini. A three-dimensional model describing stress-temperature induced solid phase transformations: solution algorithm and boundary value problems. *Int. J. of Numer. Meth. Eng.*, 2004, 6, 807-836.
[14] F. Auricchio, A. Coda, A. Reali, M. Urbano. SMA numerical modeling versus experimental results: parameter identification and model prediction capabilities. *J. Mater. Eng. Perform.*, 2009, 18, 649-654.
[15] F. Auricchio, S. Morganti, A. Reali, M. Urbano. Theoretical and Experimental Study of the Shape Memory Effect of Beam in Bending Conditions. *J. Mater. Eng. Perform.*, 2011, 20, 712-718.
[16] F. Auricchio, E. Bonetti. A new flexible 3D macroscopic model for shape memory alloys. *Discret. Contin. Dyn. Syst. Ser. S*, 2013, 6, 277-291.
[17] F. Auricchio, E. Bonetti, G. Scalet, F. Ubertini. Refined shape memory alloys model taking into account martensite reorientation. *CD-ROM Proceedings of the 6th European Congress on Computational Methods in Applied Sciences and Engineering* (ECCOMAS 2012), J. Eberhardsteiner, H.J. Bhm, F.G. Rammerstorfer (Eds), September 10-14, 2012, Wien, Austria, Vienna University of Technology, Austria, 2012, 3349-3362.
[18] AceFEM/AceGen Manual 2007, http://www.fgg.unilj.si/Symech/, 2007.
[19] M. Urbano, Al. SMAq. A Novel Instrument for the Characterization of SMA Wires. *Proceedings of the International Conference on Shape Memory and Superelastic Technologies*, May 7-11, Pacific Groove, California, USA, 2006, 177-184.
[20] Lagoudas, D. (Ed.) (2008). *Shape Memory Alloys. Modeling and Engineering Applications*. Springer.